JOURNAL OF OPTOELECTRONICS AND ADVANCED MATERIALS Vol. 10, No. 6, June 2008, p. 1401 - 1407

Highly dispersed heteropolyacids supported on modified MCM 41 mesoporous materials

A. POPA[a*], V. SASCA[a], E.E. KIŠ[b], RADMILA MARINKOVIĆ-NEDUČIN[b], J. HALASZ[c]
[a]*Institute of Chemistry Timişoara, Bl.Mihai Viteazul 24, 300223 Timisoara, Romania*
[b]*University of Novi Sad, Faculty of Technology, Cara Lazara 1, Novi Sad, Serbia*
[c]*University of Szeged, Dep.of Applied and Environmental Chemistry, Rerrich ter 1, H-6720 Szeged, Hungary*

Solid acid catalysts consisting of heteropolyacids (HPAs) $H_3PMo_{12}O_{40}$ (HPM) and $H_4PVMo_{11}O_{40}$ (HPVM) supported on mesoporous pure-silica molecular sieve MCM-41 and modified molecular sieves Al-MCM-41 and Fe-MCM-41 have been prepared and characterized by XRD, FT-IR, ^{31}P MAS NMR, low temperature nitrogen adsorption and scanning electron microscopy. All supported HPAs were prepared by impregnation using the incipient wetness techniques with a mixture water: ethanol = 1:1. FT-IR studies showed that HPAs anions preserved their Keggin structure after deposition on pure and modified molecular sieves supports. X-ray diffraction and SEM studies confirmed the uniformity of the distribution of active phase in the supported samples. The values of specific surface area of both HPAs were increased by deposition on molecular sieve supports. It is found that most of HPM and HPVM (active phases) in supported samples are well dispersed on the support and MCM-41 supported HPAs still keep its Keggin structure. The surface morphology of the MCM-41 supported samples is almost similar to that of MCM-41 support. A relatively uniform distribution of active phase in the support pores was evidenced by EDS analysis.

(Received May 12, 2008; accepted June 4, 2008)

Keywords: Heteropolyacids, Molecular sieves, Texture, structure, BET, SEM, XRD, ^{31}P MAS NMR

1. Introduction

Keggin type heteropolyacids (HPAs) have been used in acid-catalysed reactions as well as oxidation reactions both in the heterogeneous and homogeneous systems. Pure HPAs generally show low catalytic reactivity owing to their small surface area. In order to be more effective for catalytic reactions, HPAs are usually impregnated on different porous materials with high surface area [1-8].

MCM 41 mesoporous molecular sieves are very interesting materials for catalysis and as a support because they have a high thermal stability (up to 1198K), larger surface area (over 700 m^2/g) and a good adsorption capacity for organic molecules [9-22]. From preparation method and reactants types pore dimensions of MCM41 can be engineered in the range from 15 to 100 Å, which allow the easy introduction of HPAs molecules (12 Å diameter).

In the literature very few references have been reported concerning $H_3[PMo_{12}O_{40}]$ and $H_4[PMo_{11}VO_{40}]$ supported on MCM41 mesoporous silicate, majority of the studies have been focused on investigation the most acidic HPAs in the series, namely $H_3PW_{12}O_{40}$.

The catalysts Rh-HPAs supported on MCM41 prepared by impregnation of Rh complexes with $H_3PW_{12}O_{40}$ and $H_3PMo_{12}O_{40}$ for the hydroformylation of styrene derivatives have been studied by Ali and al. [15]. The choice of the solvent of impregnation was very important in order to minimize the leaching of the catalyst during reaction. The presence of HPAs with Rh(I) or Rh(III) on the support increased the catalytic activity of rhodium catalysts by improving the conversions of styrene and the recycling of the supported catalyst. Jalil and al. [18, 19] showed that HPW/Si-MCM41 composites obtained by impregnation from methanol present a dispersion of active phase more homogeneously distributed within the pores of the support than in the case of aqueous impregnation solution. Upon impregnation an interaction between the protons of HPW and hydroxyl groups of Si-MCM41 appeared and as a consequence, thermal stability of composites decreased to 400ºC, when they decompose to tungsten oxides.

By using the conversion of 1,3,5-triisopropylbenzene, the loading effect on both acidity and catalytic activity for HPW/Si-MCM41 composites was investigated [21]. Whilst an important increase in acidity and catalytic activity is observed at low loading (up to 23 wt.%), a decrease in both is found at higher loading (over 33 wt.%), the activity of composites decays to that of HPW acid. The optimum loading calculated from the ^1H NMR spectrum agrees with that found in catalytic studies. From ^1H NMR and ^{31}P NMR spectra result that at the loading of 23 wt.% HPW only ca. 80 wt.% is located inside the pores, whereas the rest of active phase is located at the entrance of the pores or at the external surface of support grains.

As a consequence of their high catalytic activity, molybdophosphoric acid $H_3[PMo_{12}O_{40}]\cdot xH_2O$ (HPM) and 1-vanado-11-molybdophosphoric acid $H_4[PMo_{11}VO_{40}]\cdot yH_2O$ (HPVM) are frequently used in the selective oxidation of unsaturated aldehydes and of low alcohols.

In order to obtain highly dispersed heteropolyacids species, HPM and HPVM were supported on Si-MCM41, Al-MCM-41 and Fe-MCM-41. The goal of this work was to characterise the texture and structure of these heteropolyacids supported on Si-MCM41 and on modified MCM-41molecular sieves.

2. Materials and methods

$H_4[PMo_{11}VO_{40}]\cdot 12H_2O$ was prepared by two methods: Tsigdinos and hydrothermal method [23-24]. In both cases HPAs were crystallized slowly from aqueous solutions at room temperature. $H_3[PMo_{12}O_{40}]\cdot 13H_2O$ was purchased from Merck. The as-received material was recrystallized prior to use. They are stable at room temperature with 12-14 H_2O molecules. Mesoporous silica Si-MCM41 and modified MCM-41molecular sieves were synthesized according to the procedure developed by Beck and colab. [9].

The HPA active phase deposition on Si-MCM41, Al-MCM-41 (Si/Al = 20) and Fe-MCM41 (Si/Fe = 50) supports was performed by impregnation from water: ethanol = 1:1 solution. The HPM and HPVM acids were deposited in the concentration of 15 and 30 wt. % loading.

The structure and texture of HPM and HPVM supported on molecular sieves were studied by XRD, FT-IR, ^{31}P MAS NMR, low temperature nitrogen adsorption and scanning electron microscopy with EDS analysis.

Textural characteristics of the outgassed samples were obtained from nitrogen physisorption using a Quantachrome instrument, Nova 2000 series. The specific surface area S_{BET}, mean cylindrical pore diameters d_p and adsorption pore volume V_{pN2} were determined. Prior to the measurements the samples were degassed to 10^{-5}Pa at 250ºC. The BET specific surface area was calculated by using the standard Brunauer, Emmett and Teller method on the basis of the adsorption data. The pore size distributions were calculated applying the Barrett-Joyner-Halenda (BJH) method to the desorption branches of the isotherms. The IUPAC classification of pores and isotherms were used in this study.

Microstructure characterisation of the catalyst particles was carried out with a JEOL JSM 6460 LV instrument equipped with an OXFORD INSTRUMENTS EDS analyser. Powder materials were deposited on adhesive tape fixed to specimen tabs and then ion sputter coated with gold. Powder X-ray diffraction data were obtained with a XD 8 Advanced Bruker diffractometer using the Cu K_α radiation in the range 2θ = 0.5-5° at low angles and 2θ = 5-60°.

The IR absorption spectra were recorded with a Jasco 430 spectrometer (spectral range 4000-400 cm^{-1} range, 256 scans, and resolution 2 cm^{-1}) using KBr pellets.

Solid-state NMR experiments were recorded on a Bruker Avance DRX 500 spectrometer equipped with a CP MAS probe. ^{31}P MAS experiments were acquired with the following parameters sets: ^{31}P $\pi/2$ pulse was 4.0 µs, 2 s repetition delays was applied and a 247.0 ppm wide spectral region was detected with a carrier placed at 0 ppm, 1 K transients were recorded in 2K complex data-points resulting in 82 ms acquisition time. Lorentzian window function (with 50 Hz broadening factor) was applied prior to all Fourier transformations. Spectra were referenced to external $NH_4H_2PO_4$ (δ_{31P} = 0 ppm).

3. Results and discussion

The XRD patterns for the initial Si-MCM41 and the two HPAs/Si-MCM41 samples are shown in Fig.1a and the data are presented in Table 1. The XRD patterns of Si-MCM41 and supported samples show three diffraction peaks below 6° (2θ): (100), (110) and (200), indicating that the long-range order of the hexagonal mesostructure is mentained after impregnation of HPAs.

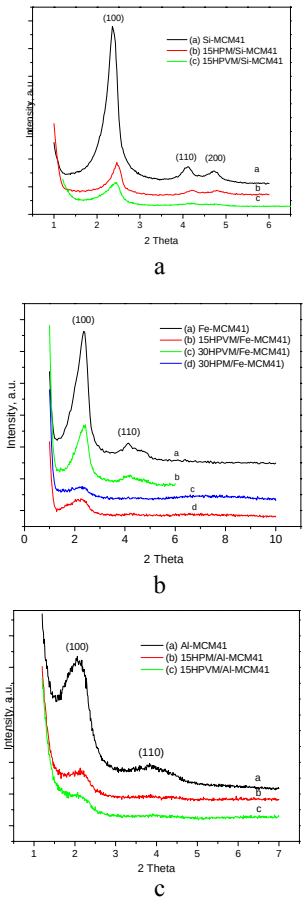

Fig. 1. X-ray diffraction pattern of Si-MCM41 (a), Fe-MCM-41 (b) and Al-MCM41 (c) molecular sieves and supported HPAs.

Fig. 1b shows the XRD patterns of Fe-MCM41 and the two HPAs/Fe-MCM41 samples. The patterns show the characteristics of a typical mesoporous MCM-41 structure. The d_{100} diffraction peaks of calcined Fe-MCM41 are shifted towards lower values compared to its Si-MCM-41 analogue. As in the case of HPW/MCM41 [12-16] the amount of HPM or HPVM has an important effect on the intensity of the main reflection peacks of the Fe-MCM14 support, and the peaks height is inversely proportional to the amount of loaded HPAs. It can be observed that the long – range order of Fe-MCM41 is decreased evidently for loading of 30 wt. % HPAs. The XRD diffraction patterns of supported HPAs do not show any bulk HPAs crystal phases, indicating that active phase is finely dispersed on the Fe-MCM41 support.

For Al-MCM41 the diffraction peaks at low angles are presented but with diminished intensity. The d_{100} diffraction peak of Al-MCM41 supported HPVM appear like a shoulder. It can be asserted that the long – range order of Al-MCM41 is decreased evidently even for loading of 15 wt. % HPAs.

The textural properties (BET surface area, pore volume and pore size) of molecular sieves and supported HPAs are shown in Table 1 and Fig. 2 and 3. All textural properties of the materials decrease with increasing HPAs loading. For example, the BET surface area and the pore volume of Si-MCM 41 (1104 m^2/g, 1.06 cm^3/g) decrease by supporting HPAs to 860 and 888 m^2/g and to 0.78 and 0.77 for HPM and HPVM, respectively.

Table 1. Textural properties of molecular sieves and supported HPAs.

Sample	XRD d_{100} d-spacing (Å)	Unit cell, a_o (nm)	Surface area (m^2/g)	Pore size BJH_{Des} (Å)	Pore volume BJH_{Des} (cc/g)
Si-MCM41	37.40	4.32	1104	25.02	1.06
15% HPM/Si-MCM41	35.88	4.14	860	25.01	0.776
15% HPVM/Si-MCM41	36.03	4.16	888	25.07	0.770
Fe-MCM41	36.78	4.25	917	26.8	0.968
15% HPVM/Fe-MCM41	36.48	4.21	769.5	24.8	0.649
30% HPVM/Fe-MCM41	36.18	4.18	655	24.2	0.685
30% HPM/Fe-MCM41	36.18	4.18	439	24.2	0.562
Al-MCM41	42.58	4.92	559.3	28.8	0.82
15% HPM/Al-MCM41	41.25	4.76	408.5	26.9	0.56
15% HPVM/Al-MCM41	42.04	4.85	364.3	26.9	0.44

The nitrogen adsorption isotherms of heteropolyacids supported on Fe-MCM-41 are shown in Figs. 2a. For 30HPVMo/ Fe-MCM-41 one observe a type IV isotherm with a type H1 hysteresis loop in the high range of relative pressure. For the values of relative pressure higher than 0.8, condensation take place giving a sharp adsorption volume increase. This behavior indicates that this sample has a mesoporous character. Hysteresis loop type shows that HPVMo/ Fe-MCM-41 sample consists of clusters or compacts of approximately uniform spheres in fairly regular array. Both HPM and HPVM heteropolyacids supported on Fe-MCM-41 present the type IV isotherm with a type H1 hysteresis loop.

The pore size distributions were calculated by Barret-Joyner-Halenda (BJH) method applied to the desorption branches of the isotherms. The pore size distribution curves of HPM and HPVM supported on Si-MCM-41 show a maximum at 2.5 nm (Figure 3a) while for HPAs supported on Fe-MCM-41 the maximum apear at ca 2.5 nm (Fig. 2b) and HPAs supported on Al-MCM-41 show a maximum at 2.7 nm (Fig. 3b).

As shown in Fig. 2b and 3 a,b, a diminution of the pore size of molecular sieves was observed after HPAs impregnation. For 30% HPAs/Fe-MCM41 samples were found the higher diminution: from 2.68 nm for Fe-MCM41 molecular sieve to 2.42 nm for 30% HPAs/Fe-MCM41 samples.

In order to confirm the presence of the Keggin anion on molecular sieves, the supported HPAs samples were analysed by FTIR. The $PMo_{12}O_{40}^{3-}$ Keggin ion structure consists of a PO_4 tetrahedron surround by four Mo_3O_{13} formed by edge-sharing octahedra. These groups are connected each other by corner-sharing oxygen. This structure give rise to four types of oxygen, being responsible for the fingerprints bands of Keggin ion between 1200 and 700 cm^{-1}.

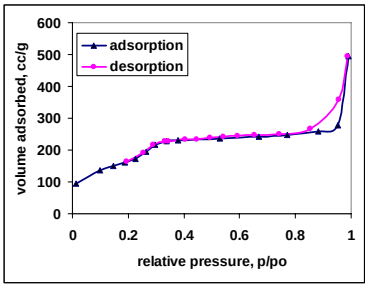

a

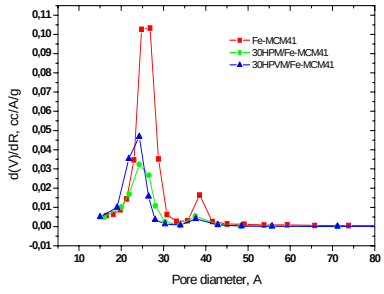

b

Fig. 2. Nitrogen adsorption-desorption isotherms of 30HPVM/ Fe-MCM-41 at 77 K (a) and pore size distribution of HPAs supported on Fe-MCM-41 (b).

The pure HPAs show an IR spectrum with the specific lines of the Keggin structure containing the main absorption lines at 1064 cm^{-1}, 965 cm^{-1}, 864 cm^{-1}, 785 cm^{-1} assigned to the stretching vibrations ν_{as} P -O, ν_{as} Mo=O_t, ν_{as} Mo-O_c-Mo and ν_{as} Mo-O_e-Mo [4, 5]. These bands are preserved on the supported samples, but they are broadened and partially obscured because of the strong absorption bands of MCM-41 (1090, 960, 800 and 465 cm^{-1}) (Fig. 4).

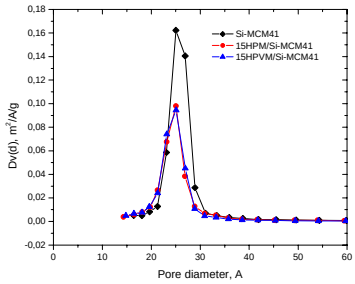

a

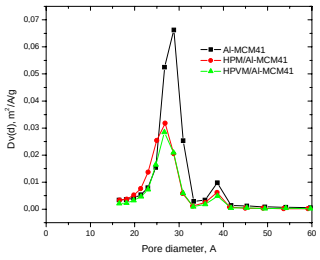

b

Fig. 3. Pore size distribution of HPAs supported on Si-MCM-41 (a) and of HPAs supported on Al-MCM-41 (b).

The introduction of Fe^{3+} and Al^{3+} cations into the Si-MCM41 support slightly influenced the structure of molecular sieve (Figure 4). The vibration band at ca. 1090 cm^{-1} can be assigned to ν_{as}(Si-O-Si) and decreased to 1086 cm^{-1} and 1084 cm^{-1} by incorporation of Fe and Al cation, respectively, into the structure of the Si-MCM41. The band at ca. 956 cm^{-1} present in the spectrum of Si-MCM41 sample can be assigned to the Si-O stretching vibration of $Si\text{-}O^{-}R^{+}$ group ($R^{+} = H^{+}$), while in the Fe-MCM41 spectra the band is shifted to 963 cm^{-1} and could be assigned to a ν_{as}(Si-O-Me) vibration. The bands at 800 and 467 cm^{-1} can be assigned to ν_s (Si-O-Si) and δ(Si-O-Si) bonds, respectively [25].

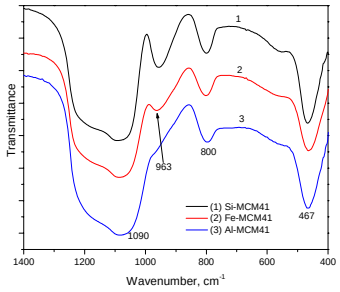

Fig. 4. FTIR spectra of Si-MCM41 molecular sieve and metal-containing molecular sieves.

Some of the bands of supported HPAs in the 1300-400 cm^{-1} region are partially or completely overlapped by the bands of the MCM41 supports (Figure 5). The band assigned to the P –O asymmetric stretching vibration at 1064 cm^{-1} is completely overlapped by the strong band at 1090 cm^{-1} of the MCM41. Two strong bands in the spectra of supported HPM and HPVM appeared at 960 and 799 cm^{-1}, as a result of the overlapping of the absorption bands of Fe-MCM41 at 963 and 801 cm^{-1} and those of HPAs at 965 and 785 cm^{-1}, respectively. Two bands with moderate intensity was observed at 562 cm^{-1} which corresponds to the bending vibration δ P-O of the HPAs and at 870 cm^{-1} which corresponds to the ν_{as} Mo-O_c-Mo band vibration which appears at 864 cm^{-1} in the HPAs spectra (Fig. 5).

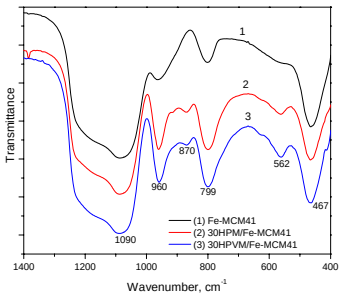

Fig. 5. FTIR spectra of Fe-MCM41 molecular sieve and supported HPAs.

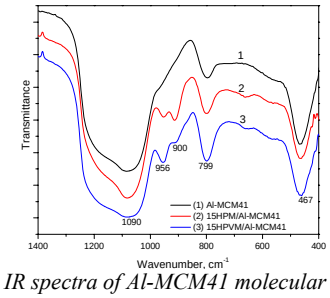

Fig. 6. IR spectra of Al-MCM41 molecular sieve and supported HPAs.

In the case of Al-MCM41 supported HPAs, the bands observed at 956 cm^{-1} which corresponds to the ν_{as} Mo=O_t band vibration and the band at 799 cm^{-1} corresponding to the ν_{as} Mo-O_e-Mo band vibration are less intense than for Fe-MCM41 supported samples (Fig. 6). The band coressponding to ν_{as} Mo-O_c-Mo which appears at 864 cm^{-1} in the HPAs spectra is shifted to 900 cm^{-1} in the spectra of Al-MCM41 supported HPAs.

Therefore, the Keggin unit would be mainly characterized by the stretching vibrations assigned to terminal Mo=O_t and bridging Mo-O_c-Mo and Mo-Oe-Mo bonds.

The replacing of a Mo atom with a V one leads to the appearance of two "shoulders" corresponding to the absorption maxim of the vibration ν_{as} (P-O_p) at 1080 cm^{-1} and ν_{as} (V-O_t) at 980 cm^{-1}. This confirms the presence of V^{5+} inside the MO_6 octahedral. These shoulders could not be seen in the IR spectra of supported HPAs as adsorption bands of silica overlap them completely.

Si-MCM41 support is composed of clusters of regular and irregular shape particles with an average diameter below 0.5 μm for smal particles and 3-5 μm for larger and regular shape particles (Fig. 7a). The surface morphology of Si-MCM41 -supported HPAs is practically identical to that of the pure molecular sieves (Fig. 7b). From SEM

images one can see that no separate crystallites of the bulk phase of HPAs were found in the supported samples.

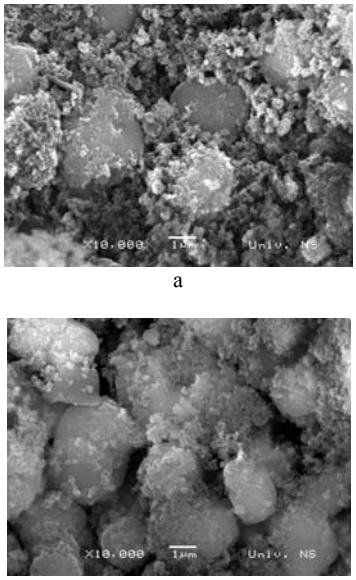

a

b

Fig. 7. SEM micrografs of Si-MCM41 (a) and HPM/ Si-MCM41 (b).

HPAs distribution on supported samples surface was analysed by EDS method, which was performed as point analysis on thin particles. By this technique were obtained the chemical composition of silicon from Si-MCM41, silicon and aluminium from Al-MCM41, silicon and iron from Fe-MCM41 and Mo, V and P elements of heteropolyacid. The EDS point analysis was made over several domains with 10x10 μm dimensions on the same sample. The analysis was repeated on different samples in order to ensure the reproducibility of the obtained results.

Microanalitycal data of EDS analysis show that the molybdenum and phosphorous (15 wt.% HPM/Si (Al, Fe)-MCM41) and molybdenum, phosphorous and vanadium (15 wt.% HPVM/Si (Al, Fe)-MCM41) content is homogeneous and close to stoichiometric values.

In the case of Al-MCM41 supported HPM the content of Mo as % wt. is 8.8 (stoichiometric value is 9.5), while P content is 0.28 (stoichiometric value is 0.25) (Figure 8 a). For Al-MCM41 supported HPVM the content of Mo as % wt. is 9.1 (stoichiometric value 8.9), P content is 0.28 (stoichiometric value is 0.26) and V content is 0.35 (stoichiometric value is 0.42).

EDS analysis of Fe-MCM41 supported HPM (30 wt. %) shows that the concentration of Mo is 17.8 wt. % (stoichiometric value is 18.9), while the P content is 0.42 wt. % (stoichiometric value is 0.50) (Fig. 8 b). It could be observed that 30HPM/ Fe-MCM41 exhibit a higher deviation of Mo and P concentration values from the stoichiometric ones, probably owing to higher active phase concentration supported at the surface of molecular sieve.

The ^{31}P MAS NMR spectra are very sensitive to to the Keggin structure symmetry and thus to its hydration state. The ^{31}P MAS NMR spectra of unsupported and supported HPMo acid on mesoporous Si-MCM41 and Al-MCM41 are shown in Fig. 9 and 10.

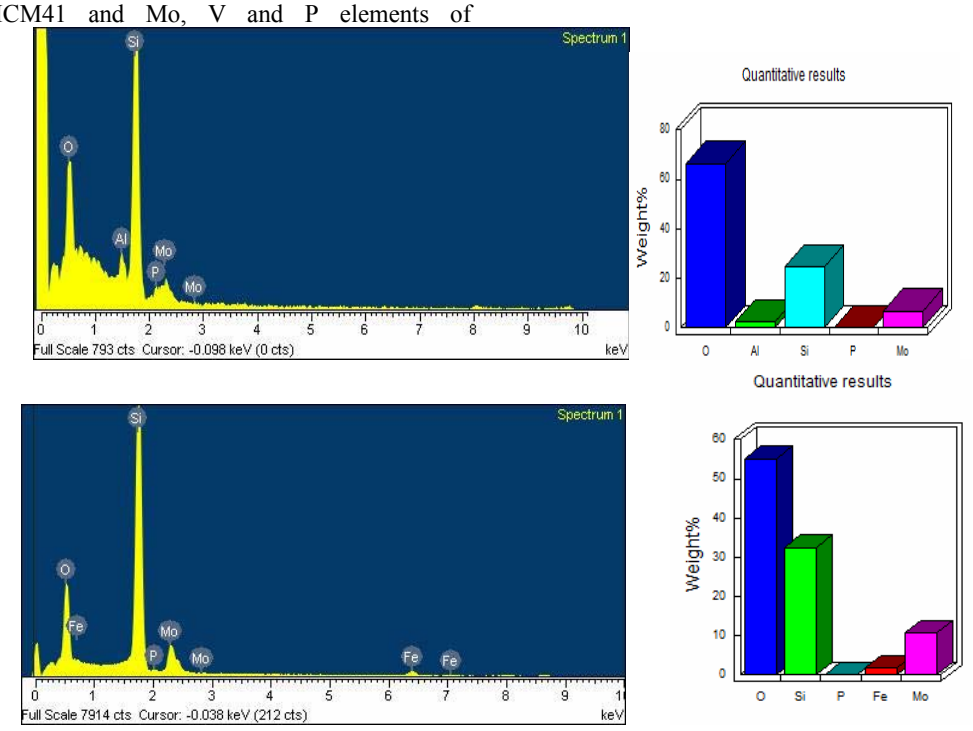

Fig. 8 a, b. Microanalytical data of a 10x10 μm area and quantitative results of 15HPM/Al-MCM41 (a) and 30HPM/ Fe-MCM41 (b).

The spectrum of crystalline HPM consists of two well-resolved peaks indicating the existence of two types of P: an intense and sharp peak at – 5.4 ppm (confirming the presence of the majority of phosphorus environment in hydrated structure of HPM acid) and a smaller one at – 5 ppm. The assignment of the smaller peak could be done to the regions of the sample having different degree of hydration [12, 21].

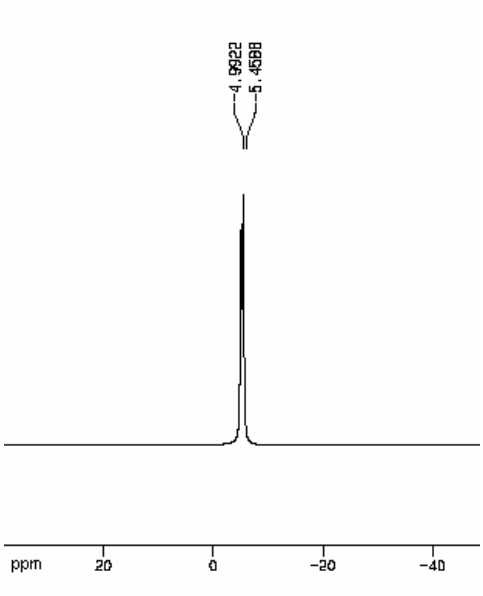

Fig. 9. ^{31}P MAS NMR of parent HPM.

After supporting the HPM on Si-MCM41 mesoporous materials, the two ^{31}P NMR peaks are preserved but broadened slightly and shifted to low field (Fig. 10a). A shift to -4.0 ppm could be observed for the peak which appears at -5 ppm in parent HPM, while the main peak slightly shifted from -5.45 ppm for HPM to -5.35 ppm for HPM/ Si-MCM41. An additional resonance at – 1.7 ppm was evidenced in the spectrum of Si-MCM41 supported HPM. This peak is shifted to down-field indicating the existence of HPM crystallites with different numbers of water molecules lost during impregnation.

The ^{31}P MAS NMR spectra of supported HPM acid on mesoporous Al-MCM41 are shown in Fig. 10b. Supporting the HPM on Al-MCM41 results in a slightly broadened of the main ^{31}P NMR peak, but resonance was preserved in the spectrum at -5.2 ppm. The broadening of the ^{31}P NMR peaks of supported samples can be attributed to a distortion of the HPAs symmetry compared with that in the crystalline form. This distortion is due to the strong chemical interaction between the heteropolyanion and the Al-MCM41 support.

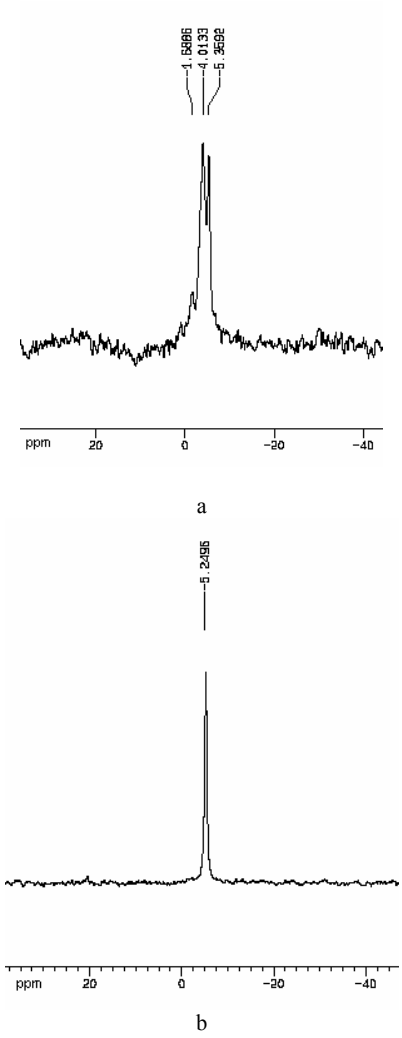

Fig. 10. ^{31}P MAS NMR of HPM supported on Si-MCM41 (a) and HPM supported on Al-MCM41.

It is known from the literature regarding supported HPAs chemistry that between active phase (HPAs) and a certain support could appear more or less strong interactions. Bruckman at al. [26] described in detail the interaction between HPAs and silica support. As molecular sieves have the same composition as silica (SiO_2) but with different distribution of the pores, the model of Bruckman for silica supported HPAs could be extended also for molecular sieves supported HPAs. At low coverage (5-15% HPA/SiO_2), when the surface of silica is sparsely populated by the Keggin units (KU) the system may be considered as composed of KU partially "immersed" in the bidimensional hydration layer at the silica surface. The bidimensional hydration layer provides a basic medium in comparison to the strong acidic heteropolyacids. Thus, in the conditions prevailing at the silica surface hydrolysis of Mo-O_c-Mo bonds (which link the triads of MoO_6 octahedra), takes place, resulting in the opening of the closed structure of the Keggin anion.

Such transformations will result in the formation of a flat structure composed of four triads linked together through the six Mo-O_c-Mo bridges and linked to the surface of silica through the PO_4 tetrahedron and some corner oxygen atoms of the triads.

As a result of these chemical interactions between the heteropolyanion and the support (silica, molecular sieves) it could be expected that the acidity of the supported HPAs diminished and such systems will show mainly redox properties.

4. Conclusions

HPAs anions preserved their Keggin structure on the Fe-MCM41 and Al-MCM41 surface and forms finely dispersed HPAs species. No HPAs detectable crystal phase is observed at 30 wt.% loading. The Fe-MCM41 host material suffers structural distortions at higher loadings, which leads to a loss in long range order.

Both Fe-MCM41 and Al-MCM41 supported HPAs exhibit differential pore size distribution in the mesoporosity range. The surface area and pore size diameter of supported HPAs decreases with increase in HPAs loading due to the partial blockage of the mesopores of molecular sieve by HPAs particles.

Keggin structure of HPAs is preserved on the Fe-MCM41 and Al-MCM41 supports, as evidenced by the agreement between the IR bands of parent and supported HPAs. The data of EDS analysis show that the molybdenum and phosphorous (HPM/Si (Al, Fe)-MCM41) and molybdenum, phosphorous and vanadium (HPVM/Si (Al, Fe)-MCM41) content is homogeneous and close to stoichiometric values.

The broadening of the ^{31}P NMR peaks of supported samples is attributed to a distortion of the HPAs symmetry compared with that in the crystalline form. This distortion is due to the strong chemical interaction between the heteropolyanion and the Si (Al, Fe)-MCM41 supports.

Acknowledgements

These investigations were financed by the Roumanian Ministry of Education and Research, Grant CNCSIS No. 78 GR/2007 and by the Serbian Ministry of Sciences, Grant OI 142024.

References

[1] F. Cavani, Catal. Today **41,** 73 (1998).
[2] N. Mizuno, M.Misono, Chem. Rev. **98,** 199 (1998).
[3] M. Misono, Catal. Rev. -Sci. Eng. **29,** 269 (1987).
[4] A. Popa, V. Sasca, E. E. Kiss, Radmila Marinkovic-Neducin, M. T. Bokorov, J. Halasz, J. Optoelectron. Adv. Mater. **7**(6), 3169 (2005).
[5] A. Popa, V. Sasca, M. Stefănescu, E. E. Kis, R. Marinkovic-Neducin, J. Serb. Chem. Soc**. 71**(3), 235 (2006).
[6] A. Popa, V. Sasca, Radmila Marincovic-Neducin and Erne.E.Kis, Rev. Roum.Chim. **51**(3), 211 (2006).
[7] A. Popa, Nicoleta Pleşu, V. Sasca, E. E. Kiš, Radmila Marinković-Nedučin, J. Optoelectron. Adv. Mater. **8**(5)**,** 1944 (2006).
[8] A. Popa, V. Sasca, E. E. Kiss, Radmila Marinkovic-Neducin, J. Halasz, J. Optoelectron. Adv. Mater. **9**(11), 3645 (2007).
[9] J. S. Beck, J. C. Vartuli, W. J. Roth, M. E. Leonowicz, C. T. Kresge, K .D. Schmitt, C. T- W. Chu, D. H. Olson, E. W. Sheppard, S. B. McCullen, J. B. Higgins, J. L. Schlenker, J. Am. Chem. Soc. **114,** 10834 (1992).
[10] K. Murata, Y. Liu, N. Mimura, M. Inaba, Catal. Comm. **4**, 385 (2004).
[11] Y. Luo, G. Z. Lu, Y. L. Guo, Y. S. Wang, Catal. Comm. **3**, 129 (2002).
[12] I. V. Kozhevnikov, A. Sinnema, R. J. J. Jansen, K. Pamin, H. van Bekkum, Catal. Lett. **30**, 241 (1995).
[13] W. Chu, X. Yang, Y. Shan, X. Ye, Y. Wu, Catal. Lett. **42**, 201 (1996).
[14] S. Udayakumar, S. Ajaikumar, A. Pandurangan, Appl. Catal. A: General **302**, 86 (2006).
[15] B. E. Ali, J. Tijani, M. Fettouhi, M. E. Faer. A. A. Arfaj, Appl. Catal. A: General **283**, 185 (2005).
[16] R. R. Jermy, A. Pandurangan, Appl. Catal. A: General, **295**, 185 (2005).
[17] R. Maheswari, K. Shanthi, T. Sivakumar, S. Narayanan, Appl. Catal. A:General, **248**, 291 (2003).
[18] P. A. Jalil, M. A. Al-Daous, A. R. A. Al-Arfaj, A. M. Al-Amer, J. Beltramini, S. A. I. Barri, Appl. Catal. A: General, **207**, 159 (2001).
[19] P. A. Jalil, N. Tabet, M. Faiz, N. M. Hamdan, Z. Hussain, Appl. Catal. A:General, **257**, 1 (2004).
[20] K. Nowinska, W. Kaleta, Appl. Catal. A:General **203**, 91 (2000).
[21] A. G. Siahkali, A. Philippou, J. Dwyer, M. W. Anderson, Appl. Catal. A:General **192**, 57 (2000).
[22] M. J. Verhoef, P. J. Kooyman, J. A. Peters, H. van Bekkum, Microporous Mesoporous Mater. **27**, 365 (1999).
[23] G. A. Tsigdinos, Inorg. Chem. **7**, 437 (1968).
[24] F. Kern, St. Reif, G. Emig, Appl. Catal., **150**, 143 (1997).
[25] S. C. Laha, P. Mukherjee, S. R. Sainkar, R. Kumar, J.Catal.. **207**, 213 (2002).
[26] K. Bruckman, M. Che, J. Haber, J. M. Tatibouet, Catal. Lett. **25**, 225 (1994).

*Corresponding author: alpopa_tim2003@yahoo.com